

tem  $Gd_xZr_{1-x}Zn_2$ . More than that, our calculations indicate that the observed maximum in  $\Delta H$  and minimum in  $\Delta g$  are not explained by the existence of a bottleneck effect.

<sup>19</sup>Our experimental results indicate that the total line-width in  $Gd_xZr_{1-x}Zn_2$  increases with the increase of Gd concentration (at low temperatures). This behavior is

probably due to Gd-Gd interaction as well as to demagnetization effects. We therefore attribute the differences between the theoretical and experimental results for the sample  $Gd_{0.06}Zr_{0.94}Zn_2$  to this effect.

<sup>20</sup>D. Shaltiel, D. Davidov, G. Dublon, A. Gabai, and A. Grill, International Conference on Magnetism, Grenoble, 1970 (unpublished).

## Transverse-Magnetization Recovery in the Rotating Frame\*

Won-Kyu Rhim<sup>†</sup> and Horst Kessemeier

*Department of Physics, University of North Carolina, Chapel Hill, North Carolina 27514*

(Received 12 March 1970; revised manuscript received 12 February 1971)

The transverse relaxation of  $F^{19}$  nuclei in Teflon in the rotating frame at exact resonance has been studied by using rf fields large compared to the local field in this solid. Various pulse sequences are explored which serve to trace out the decay of the magnetization in the rotating frame and, further, to recover the magnetization lost under the action of secular dipolar terms and of the inhomogeneity of the rf magnetic field. It is found theoretically, and partially confirmed experimentally, that the rotary free-induction decay can be refocused even after the spin system has presumably attained a steady state in the rotating frame, contrary to the assumption of the spin-temperature approximation.

### I. INTRODUCTION

A nuclear resonance signal in the presence of a strong rf magnetic field at right angles to the dc magnetic field cannot be observed directly. Instead, the height of the free-induction decay (FID) following an rf pulse of length  $\tau$  has to be recorded and related to the magnetization existing at time  $\tau$ . Two procedures are available which permit the tracing out of the FID in the tilted rotating frame by recording the FID in the laboratory frame.

(i) An rf pulse of variable length  $\tau$  is followed by a  $90^\circ$  sampling pulse at time  $t_d$  later with  $t_d$  satisfying the condition  $T_2 \ll t_d \ll T_1$ . If a laboratory system of coordinates is chosen with its  $z$  axis along the direction of the dc field and its  $x$  axis along the rf field, then this pulse sequence represents a measure of the  $z$  component of magnetization  $M_z(\tau)$ . In this fashion, Goldburg and Lee<sup>1</sup> have measured the rotary FID in a single crystal of  $CaF_2$  and found that at exact resonance the decay envelope of  $M_z(\tau)$  approximately coincides with the laboratory FID with its time scale expanded by a factor of 2.

(ii) Similarly, one should suppose, the component of magnetization in the  $x, y$  plane, say,  $M_y(\tau)$ , can be determined directly by reading the height of the FID following the rf pulse of length  $\tau$ . Barnaal and Lowe<sup>2</sup> have measured as a function of  $\tau$  the variation in the positions of the zero points of the FID in single crystals of  $CaF_2$  and gypsum. For pulse lengths of up to  $20 \mu\text{sec}$ , they demonstrated the expected line narrowing by a

factor of 2 at exact resonance with considerable accuracy.

We have simultaneously measured both components of magnetization of the  $F^{19}$  resonance in Teflon at exact resonance for longer pulse widths and found that the rotary-decay envelopes differ both in width and shape, contrary to the expectation of a precessing and dephasing magnetization in the tilted rotating frame. The purpose of the present investigation is therefore twofold, namely, (i) to present a calculation accounting for this discrepancy, and (ii) to lock or recover the magnetization by means of various pulse sequences which existed at the time of shutoff of the rf pulse.

An important implication of the calculation is that the isolated spin system does not attain a state of internal equilibrium in the presence of a strong rf field contrary to the assumption of the spin-temperature approximation. The magnetization which has dephased under the action of the secular dipolar coupling may, under certain conditions, be recovered independently of the length of the rf pulse.

A theoretical analysis of these phenomena is presented in Sec. II. The experimental results are reported and discussed in Sec. III, and Sec. IV contains a summary of this investigation.

### II. THEORETICAL CONSIDERATIONS

Consider a sample containing  $N$  identical nuclei having spin  $\bar{I}$  and gyromagnetic ratio  $\gamma$ . The sample is exposed to a dc magnetic field  $\bar{H}_0$  pointing along the  $z$  axis of a laboratory system of coordinates

and an rf field  $2\tilde{H}_1 \cos\omega t$  along the  $x$  axis. We shall assume that the internuclear coupling is correctly described by the truncated dipolar interaction both in the laboratory system  $(x, y, z)$  and in the tilted rotating frame  $(X, Y, Z)$ . The latter assumption implies that  $H_1$  is large compared to the local dipolar field such that all nonsecular terms may be neglected.

The Hamiltonian of the spin system in the laboratory frame is then given by

$$\mathcal{H} = \hbar[-\gamma(\tilde{H}_0 + 2\tilde{H}_1 \cos\omega t) \cdot \tilde{I} + \mathcal{H}_0], \quad (1)$$

where

$$\mathcal{H}_0 = \sum_{i < j} B_{ij}(I_{zi}I_{zj} - \frac{1}{3}\tilde{I}_i \cdot \tilde{I}_j),$$

with

$$B_{ij} = \frac{3}{2}\gamma^2\hbar(1 - 3\cos^2\theta_{ij})/r_{ij}^3,$$

and in the rotating frame at exact resonance,

$$\mathcal{H}_{\text{er}} = \hbar(-\omega_1 I_x + \mathcal{H}_0). \quad (2)$$

A unitary transformation of  $\mathcal{H}_{\text{er}}$  yields the Hamiltonian in a frame tilted about the  $y$  axis through an angle  $\theta = \pi/2$  such that  $\tilde{H}_1$  is parallel to the new  $Z$  axis.<sup>3</sup> Let  $S = e^{-i(\pi/2)I_y}$ , then

$$\mathcal{H}_T = (S^{-1}\mathcal{H}_{\text{er}}S)/\hbar = -\omega_1 I_z + \lambda_0(\theta)\hat{\mathcal{H}}_0, \quad (3)$$

where

$$\hat{\mathcal{H}}_0 = \sum_{i < j} B_{ij}(I_{zi}I_{zj} - \frac{1}{3}\tilde{I}_i \cdot \tilde{I}_j),$$

and, at exact resonance,  $\lambda_0(\theta) = \frac{1}{2}(3\cos^2\theta - 1) = -\frac{1}{2}$ .

#### A. Relationship between the Rotary and Laboratory FID Envelopes

In order to trace out the FID in the presence of an rf field by recording the FID immediately following the rf pulse, it is necessary to relate the signal amplitudes in the two frames of reference. It will be instructive to consider first the FID following an instantaneous  $90^\circ$  rf pulse applied along the  $x$  axis at time  $t = 0$ .

The normalized decay envelope in the high-temperature approximation is given by the correlation function<sup>4</sup>

$$G(t) = \text{Tr}(I_y e^{-i\mathcal{H}_{\text{er}}t/\hbar} I_y e^{i\mathcal{H}_{\text{er}}t/\hbar}) / \text{Tr}I_y^2. \quad (4)$$

Using the identity for any two operators  $A$  and  $B$ ,<sup>5</sup>

$$e^A B e^{-A} = \sum_{n=0}^{\infty} \frac{1}{n!} \tilde{A}^n B, \quad (5)$$

where

$$\tilde{A}^n B = [A, [A, \dots, [A, B] \dots]],$$

$G(t)$  can be expanded as

$$G(t) = 1 + \frac{t^2}{2!} \frac{\text{Tr}[(\tilde{\mathcal{H}}_0 I_y)^2]}{\text{Tr}I_y^2} + \frac{t^4}{4!} \frac{\text{Tr}[(\tilde{\mathcal{H}}_0^2 I_y)^2]}{\text{Tr}I_y^2} + \dots$$

$$= 1 - \frac{t^2}{2!} M_2 + \frac{t^4}{4!} M_4 + \dots, \quad (6)$$

where  $M_2$  and  $M_4$  are the second and fourth moments of the absorption line, and all odd moments vanish.<sup>4</sup>

If the rf pulse now has a length  $\tau$  and the signal is observed at time  $\tau_1$  measured from the end of the pulse, one has, instead of (4),

$$V(\tau + \tau_1) = \frac{1}{\text{Tr}I_y^2} \text{Tr}(I_y \tilde{e}^{i\mathcal{H}_0\tau_1} e^{-i(\mathcal{H}_{\text{er}}/\hbar)\tau} \times I_x e^{i(\mathcal{H}_{\text{er}}/\hbar)\tau} e^{i\mathcal{H}_0\tau_1}). \quad (7)$$

The value of the trace is invariant under a rotation by  $\pi/2$  around the  $y$  axis. Let  $S = e^{-i(\pi/2)I_y}$ , then

$$V(\tau + \tau_1) = \frac{-1}{\text{Tr}I_y^2} \text{Tr}[S^{-1}(e^{i\mathcal{H}_0\tau_1} I_y e^{-i\mathcal{H}_0\tau_1}) \times (e^{i\mathcal{H}_T\tau} I_x e^{i\mathcal{H}_T\tau})], \quad (8)$$

with

$$e^{-i\mathcal{H}_T\tau} I_x e^{i\mathcal{H}_T\tau} = e^{i\mathcal{H}_0\tau/2} (I_x \cos\omega_1\tau - I_y \sin\omega_1\tau) e^{-i\mathcal{H}_0\tau/2},$$

since  $[I_z, \hat{\mathcal{H}}_0] = 0$ .

We are interested in the envelope of the decaying magnetization. Therefore, we are considering only  $\tau$ 's which define maxima of the sinusoidally varying signal, i. e.,  $\tau$  should satisfy the condition

$$\omega_1\tau = \frac{1}{2}\pi + n\pi \quad (n = 0, 1, 2, \dots). \quad (9)$$

Then, (8) simplifies to

$$V(\tau + \tau_1) = \frac{(-1)^n}{\text{Tr}I_y^2} \text{Tr}[S^{-1}(e^{i\mathcal{H}_0\tau_1} I_y e^{-i\mathcal{H}_0\tau_1}) \times S(e^{-i\mathcal{H}_0\tau/2} I_y e^{i\mathcal{H}_0\tau/2})]. \quad (10)$$

Using the equality  $[S^{-1}\mathcal{H}_0S, I_y] = -[\hat{\mathcal{H}}_0, I_y]$ , an expansion of (10) as defined by (5) yields

$$V(\tau + \tau_1) = (-1)^n \left\{ \left[ 1 - \frac{1}{2!} \left( \frac{\tau}{2} + \tau_1 \right)^2 M_2 + \frac{1}{4!} \left( \frac{\tau}{2} + \tau_1 \right)^4 M_4 + \dots \right] - \frac{6}{4!} \left( \frac{\tau}{2} \right)^2 \tau_1^2 M_{4x} + \dots \right\}, \quad (11)$$

where

$$M_{4x} = \frac{\text{Tr}\{[(\hat{\mathcal{H}}_0 + S^{-1}\mathcal{H}_0S), [\hat{\mathcal{H}}_0, I_y]][\hat{\mathcal{H}}_0, [\mathcal{H}_0, I_y]]\}}{\text{Tr}I_y^2}, \quad (12)$$

and  $M_2$  and  $M_4$  are as defined by Eq. (6) with  $\mathcal{H}_0$

replaced by  $\mathcal{K}_0$ .

Equation (11) permits the following conclusions:

(i) If  $\tau_1 = 0$ , the error term [the last term in (11)] vanishes, and the terms inside the square brackets are identical to those in Eq. (6) for a FID following a  $90^\circ$  rf pulse applied in the laboratory frame, except that  $t$  is replaced by  $\tau/2$ . In fact, a comparison of Eqs. (4) and (10) shows that all the higher terms should also be identical.

(ii) If  $\tau_1 \neq 0$ , and we suppose  $M_{4x} = 0$ , then the signal following the rf pulse should be a continuation of the laboratory FID starting at  $t = \tau/2$ . This confirms the results predicted by Barnaal and Lowe.<sup>2</sup> The pulse lengths they used were less than  $20 \mu\text{sec}$  so that the error term might not have been large enough to affect the positions of the zero points.

It should be pointed out that  $V(\tau + \tau_1)$  can be expressed as

$$V(\tau + \tau_1) = G\left[\frac{1}{2}(\tau + 2\tau_1)\right], \quad (13)$$

where  $G(t)$  is defined in Eq. (4) with  $M_{4x}$  neglected. This means that the time scale of  $G(t)$  should be stretched by a factor of 2 and shifted to the left by  $2\tau_1$  if the signal amplitude is measured at  $t = \tau + \tau_1$ . Several experimental techniques will be introduced which eliminate the error term by effectively making  $\tau_1 = 0$ .

(iii) The error term is proportional to  $\tau^2$  for a given  $\tau_1 \neq 0$  thus affecting the shape of the signal more seriously as the rf pulse length is increased.  $M_{4x}$  is found to be identical to the corresponding error term in the calculation of Powles and Strange<sup>6</sup> for a  $(90^\circ)_{\text{rf}} \sim \tau \sim (90^\circ)_{90^\circ} \sim \tau'$  pulse sequence. Replacing the time parameters  $\tau' \rightarrow \frac{1}{2}\tau$ , and  $\tau \rightarrow -\tau_1$  in their trace for  $V(\tau + \tau')$  [Eq. (9) of Ref. 6], the trace becomes identical to Eq. (10).

Powles and Strange<sup>6</sup> and Mansfield<sup>7</sup> calculated  $M_{4x}$  for a simple-cubic lattice with lattice constant  $d$  for the static magnetic field along the [100] direction. Considering only dipolar interactions similar to our case, they found

$$M_{4x} = -3M_2^2[0.46 - 0.021/I(I+1)], \quad (14)$$

with

$$M_2 = (36.8/d^6)\gamma^2\hbar(1 - 0.187)\frac{1}{3}I(I+1).$$

Comparison of (14) with  $M_4$  shows that, in general,  $-M_{4x} < M_4$ .

#### B. Measurement of $M_y(t)$ for a $(\tau)_{\text{rf-x}} \sim \tau_1 \sim (90^\circ)_{\text{rf-y}} \sim \tau_2$ Pulse Sequence at Exact Resonance

An important technique for recovering magnetization dephased by the action of the secular dipolar interaction in the rotating frame consists of the following pulse sequence. An rf pulse of length  $\tau$  is applied along the  $x$  axis followed by a  $90^\circ$ -

phase-shifted  $90^\circ$  pulse at time  $\tau_1$  after the first pulse has been turned off [see Fig. 2(b)].  $M_y(t)$  will be observed at time  $\tau_2$  after the second rf pulse.

The normalized signal in the first rotating frame, then, is from (7)

$$V(\tau + \tau_1 + \tau_2) = \frac{1}{\text{Tr}I_y^2} \text{Tr}(I_y e^{-i\mathcal{K}_0\tau_2} S^{-1} e^{-i\mathcal{K}_0\tau_1} e^{-i(\mathcal{K}_{\text{er}}/\hbar)\tau} \times I_x e^{i(\mathcal{K}_{\text{er}}/\hbar)\tau} e^{i\mathcal{K}_0\tau_1} S e^{i\mathcal{K}_0\tau_2}); \quad (15)$$

and in the tilted frame with (3)

$$V(\tau + \tau_1 + \tau_2) = \frac{1}{\text{Tr}I_y^2} \text{Tr}[S(e^{i\mathcal{K}_0\tau_2} I_y e^{-i\mathcal{K}_0\tau_2}) S^{-1} e^{-i\mathcal{K}_0\tau_1} \times S e^{i\mathcal{K}_0\tau/2} e^{i\omega_1 I_z \tau} I_x e^{-i\omega_1 I_z \tau} e^{-i\mathcal{K}_0\tau/2} S^{-1} e^{i\mathcal{K}_0\tau_1}]. \quad (16)$$

For  $\tau$ 's which satisfy condition (9)

$$V(\tau + \tau_1 + \tau_2) = \frac{(-1)^n}{\text{Tr}I_y^2} \text{Tr}[S(e^{i\mathcal{K}_0\tau_2} I_y e^{-i\mathcal{K}_0\tau_2}) S^{-1} e^{-i\mathcal{K}_0\tau_1} \times S(e^{i\mathcal{K}_0\tau/2} I_y e^{-i\mathcal{K}_0\tau/2}) S^{-1} e^{i\mathcal{K}_0\tau_1}]. \quad (17)$$

After some algebraic manipulations, the trace can be reduced to the following form including up to fourth-order terms in  $\tau$ ,  $\tau_1$ , and  $\tau_2$ :

$$V(\tau + \tau_1 + \tau_2) = (-1)^n \left[ \left( 1 - \frac{(\frac{1}{2}\tau + \tau_1 - \tau_2)^2}{2!} M_2 + \frac{(\frac{1}{2}\tau + \tau_1 - \tau_2)^4}{4!} M_4 + \dots \right) - \frac{6}{4!} \tau_1 \left[ \left( \frac{1}{2}\tau \right)^2 (\tau_1 - 2\tau_2) + (\tau + \tau_1)\tau_2^2 \right] M_{4x} + \dots \right]. \quad (18)$$

Equation (18) allows the following observations:

(i) If  $\tau_1 = 0$ , an echo should be formed centered at  $\tau_2 = \frac{1}{2}\tau$  which traces out the complete rotary-decay envelope of  $M_y(\tau)$  compressed in time by 2. The spin system, of course, is considered to be isolated. The pulse length is restricted to values of  $\tau = \frac{1}{2}\pi + n\pi$ , where  $n$  may be an arbitrarily large integer, and the refocussing  $90^\circ$  pulse should follow instantaneously ( $\tau_1 = 0$ ) and be phase shifted by  $90^\circ$  with respect to the leading rf pulse. With these restrictions in mind, the rotary echo may be considered as a consequence of the sign reversal and multiplication by  $\frac{1}{2}$  of the doubly truncated Hamiltonian in going from the rotating frame [Eq. (2)] to the tilted rotating frame [Eq. (3)], effectively reversing time.

(ii) If  $\tau_1 \neq 0$ , the echo maxima will be observed at  $\tau_2 = \frac{1}{2}\tau + \tau_1$  with amplitude given by

$$V(\frac{3}{2}\tau + 2\tau_1) = (-1)^n [1 - (6/4!) \tau_1^2 (\tau + \tau_1)^2 M_{4x}], \quad (19)$$

i. e., the echo maximum will be decreased by  $(6/4!) \tau_1^2 (\tau + \tau_1)^2 M_{4x}$ .

(iii) If  $\tau_1 = \tau_2$ ,

$$V(\tau + 2\tau_1) = (-1)^n \left[ \left( 1 - \frac{(\frac{1}{2}\tau)^2}{2!} M_2 + \frac{(\frac{1}{2}\tau)^4}{4!} M_4 + \dots \right) + \frac{3}{4!} \tau_1^2 (\frac{1}{2}\tau - \tau_1)^2 M_{4x} + \dots \right]. \quad (20)$$

A change in sign of the error term should be noted. Equation (20) shows that for short  $\tau_1$ , or for  $\tau_1$  of the order of  $\tau/2$ , the error term is negligibly small, leaving a result which is identical to Eq. (11) with  $\tau_1 = 0$ .

### III. EXPERIMENTAL RESULTS AND DISCUSSION

All experiments reported here were conducted at 45 MHz on the  $F^{19}$  resonance in Teflon at room temperature. Its characteristic relaxation times ( $T_2 \approx 33 \mu\text{sec}$ ,  $T_1 \approx 250 \text{msec}$ ) made it suitable for testing various line-narrowing procedures in the rotating frame. Unless otherwise stated, the rf inhomogeneity across the sample amounted to about 2% of  $H_1$  and thus did not broaden the rotary line shapes at exact resonance within experimental accuracy. The experimental results will be described according to the combination of rf pulses used.

(i) The rotary component  $M_x(t)$  of magnetization was measured by means of the Goldburg-Lee sequence.<sup>1</sup> An rf pulse of variable length  $\tau$  was applied followed by a  $90^\circ$  sampling pulse at time  $t_d$  later, with  $t_d$  satisfying the condition  $T_2 \ll t_d \ll T_1$ . During the time interval  $t_d$ , the transverse component of the precessing magnetization around  $H_0$  will have completely decayed leaving only the component parallel to  $H_0$ . The signal amplitude following the sampling pulse was recorded as a function of the first pulse length  $\tau$ .

The observed maxima and minima of  $M_x(t)$  are plotted in Fig. 1 for two values of  $H_1$  and are compared with the normalized laboratory FID stretched in time by a factor of 2. The hidden portion of the signal inside the 8- $\mu\text{sec}$  receiver blocking time was assumed to have a Gaussian shape. In spite of the error which might arise in the extrapolation process, the agreement between the data is good.

Instead of measuring  $M_x(t)$  it should also be possible to determine directly the rotary component of magnetization  $M_y(t)$  in the  $x, y$  plane by recording the amplitude of the FID immediately following the first rf pulse. It was believed that this signal could be matched without distortion to the beginning portion of the decay function  $G(t)$  in the laboratory frame. If this is true, then the measurement of  $M_y(t)$  obtained by reading the signal amplitude at the point  $t = \tau + \tau_1$  ( $\tau_1$  is larger than the receiver

blocking time) will be proportional to the decay function  $G[\frac{1}{2}(\tau + 2\tau_1)]$ . Namely, the observed decay of  $M_y(t)$  should be narrowed by a factor of 2 as compared to the laboratory FID but shifted to the left by  $2\tau_1$ . Barnaal and Lowe<sup>2</sup> have confirmed this result for rf pulse lengths of up to 20  $\mu\text{sec}$ .

We have extended these measurements toward longer pulse widths  $\tau$  by recording the signal amplitudes in Teflon 15  $\mu\text{sec}$  after shutoff of the rf pulse as a function of  $\tau$ . The normalized decay function  $G[\frac{1}{2}(\tau + 2\tau_1)]$  is plotted in Fig. 1 and compared with the measured maximum and minimum values of  $M_y(t)$ . The discrepancy between these two decay curves is outside the experimental error. Several sets of data were taken for different values of  $H_1$ , but the results show this discrepancy consistently, with the measured  $M_y(t)$  decaying more rapidly than  $G[\frac{1}{2}(\tau + 2\tau_1)]$ . Furthermore, and more importantly, the decay shapes are different.

Taking into account only the secular part of the dipolar Hamiltonian in the tilted rotating frame, we have computed  $M_y(t)$  for  $\tau_1 \neq 0$  [Eq. (11)] up to fourth order in  $\tau$  and  $\tau_1$  and found a discrepancy between the two components of magnetization in the fourth-order term. This error term, and those in higher order, then falsify a direct measurement of the actual time-dependent behavior of  $M_y(t)$ . It should be emphasized that  $M_y(t)$  and  $M_x(t)$  would be identical if it were possible to observe the signal immediately after the first rf pulse is turned off (i. e., for  $\tau_1 = 0$ ). The calculation shows that the error term increases proportionally to  $\tau^2$  for a given  $\tau_1$ . The experimental results indicate that for large values of  $\tau$  the difference between the two decay curves again decreases. This fact may be explained by noticing that error terms in even higher order should become important as  $\tau$  becomes large.

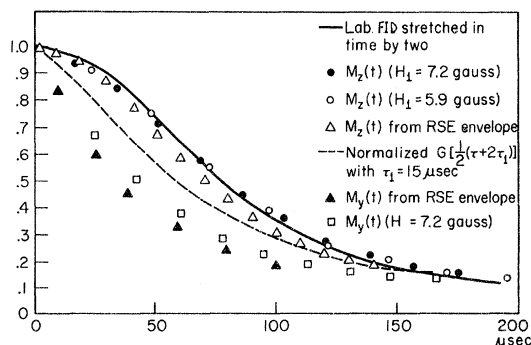


FIG. 1. Normalized decay envelope points of the rotary-magnetization components  $M_x(t)$  and  $M_y(t)$  [(i) of Sec. III]. Rotary spin-echo (RSE) envelopes obtained by  $180^\circ$  phase inversion at the midpoint of an inhomogeneous rf field [(v) of Sec. III] are plotted for comparison.

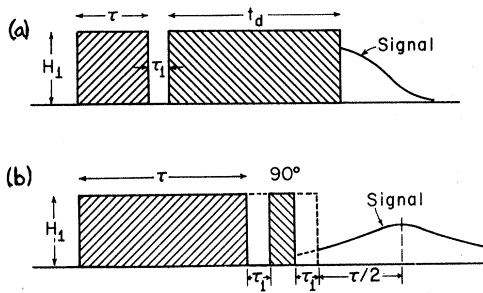


FIG. 2. (a) Locking sequence [(ii) of Sec. III]. The second rf pulse is shifted in phase by  $90^\circ$  with respect to the first pulse.  $\tau$  is arbitrary, and  $t_d$  is chosen such that  $T_{2p} \ll t_d \ll T_{1p}$ . (b) Time-inversion sequence [(iii) and (iv) of Sec. III]. The  $90^\circ$  pulse is phase shifted by  $90^\circ$  with respect to the rf field. The pulse length is restricted to values of  $\tau = \pi/2 + n\pi$ , where  $n$  is an integer.

(ii) In order to establish agreement between the results in (i), the pulse sequence of Fig. 2(a) was chosen which effectively removes the receiver blocking time. The first rf pulse of variable length  $\tau$  is immediately followed by a  $90^\circ$  phase-shifted long rf pulse of fixed length  $t_d$ . The amplitude of the signal following the second rf pulse was measured as a function of  $\tau$ .  $t_d$  was chosen to satisfy  $T_{2p} \ll t_d \ll T_{1p}$ , where  $T_{2p}$  and  $T_{1p}$  are, respectively, the transverse and longitudinal relaxation times in the tilted rotating frame. At the end of the time interval  $t_d$ , the transverse components of magnetization with respect to  $H_1$  will have completely decayed, leaving only the com-

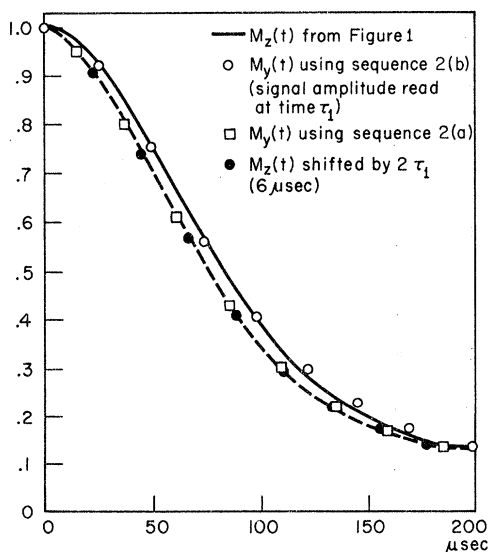
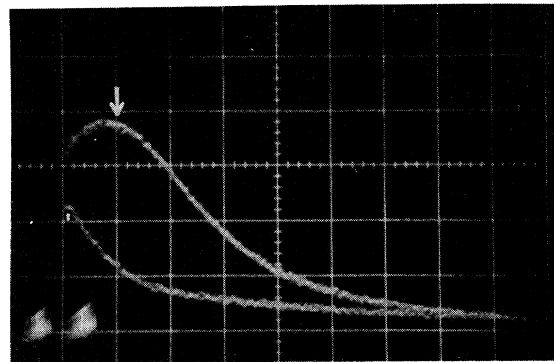
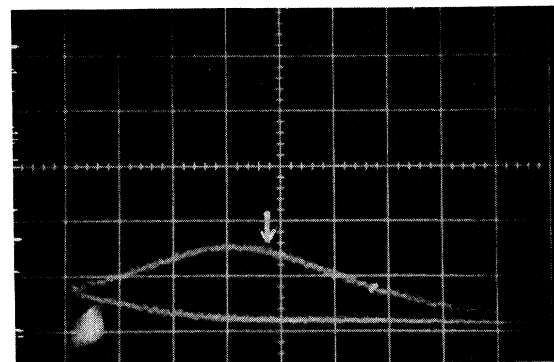


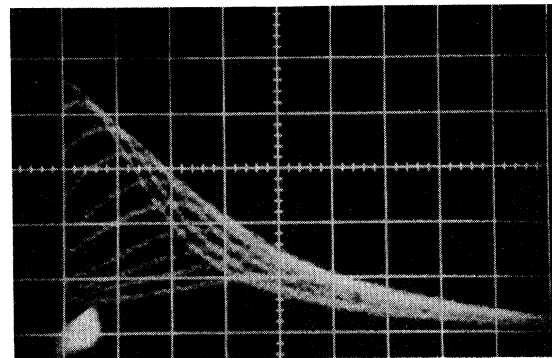
FIG. 3. Normalized rotary-decay envelope of  $M_y(t)$  obtained by applying either pulse sequence of Fig. 2(a) or 2(b) [(ii) and (iii) of Sec. III].  $H_1 = 5.72$  G.  $M_z(t)$  from Fig. 1 is plotted for comparison.



(a)



(b)



(c)

FIG. 4. Echoes in Teflon at exact resonance generated by pulse sequence of Fig. 2(b) [(iv) of Sec. III]. The oscilloscope sweep rate is  $20 \mu\text{sec}/\text{cm}$ . Arrows indicate the theoretically expected positions of the echo maxima. (a) Upper trace: echo for  $n=2$ ; lower trace: signal without refocussing pulse. (b) Upper trace: echo for  $n=7$ ; lower trace: signal without refocussing pulse. (c) Multiple exposure of echoes from  $n=0$  to  $n=9$ .

ponent along  $H_1$ . This technique is similar to the spin-locking method used by Hartmann and Hahn<sup>8</sup> and Slichter *et al.*,<sup>9,10</sup> as it effectively locks the component of magnetization parallel to  $H_1$  which existed at the time when the first rf pulse was turned off.

Figure 3 shows the experimental data points  $M_y(t)$  so obtained using  $H_1 = 5.72$  G and  $t_d \approx 440$   $\mu$ sec. Therefore, the condition  $T_{2p} \ll t_d \ll T_{1p}$  was satisfied ( $T_{2p} \approx 65$   $\mu$ sec and  $T_{1p} \approx 2.05$  msec).  $M_y(t)$  appears slightly shifted to the left with respect to the envelope of  $M_x(t)$  from Fig. 1 which was plotted for comparison. A pulse separation of about 3  $\mu$ sec could be achieved experimentally. If one shifts  $M_x(t)$  by  $2\tau_1 = 6$   $\mu$ sec to the left, the agreement between two decay envelopes is excellent. This shows that a measurement of the signal amplitude at a point very close to the end of the first rf pulse indeed determines the decay function for both  $M_x(t)$  and  $M_y(t)$  in the rotating frame, as is, of course, expected from theory.

(iii) The pulse sequence illustrated in Fig. 2(b) shows the equivalency between  $M_x(t)$  and  $M_y(t)$  directly and thus completely removes any receiver blocking. The first rf pulse of variable length  $\tau$  is followed by a  $90^\circ$ -phase-shifted  $90^\circ$  pulse. The two pulses are separated by the time interval  $\tau_1$  which may be determined by the receiver blocking time (8  $\mu$ sec, in our case).  $\tau$  satisfies the condition  $\tau = \pi/2 + n\pi$ , where  $n$  is an integer. The signal amplitudes at time  $\tau_1 = 8$   $\mu$ sec after shutoff of the second pulse were recorded as a function of  $n$  and plotted in Fig. 3. The data points corresponding to maximum amplitudes coincide, within experimental accuracy, with the envelope of  $M_x(t)$  taken from Fig. 1.

The signal amplitude  $V(\tau + 2\tau_1)$  obtained by applying this particular pulse sequence is predicted by Eq. (20). The change in sign of the error term may cause the signal to decay slower, as might be expected from a straightforward moment expansion of the rotary FID. The expansion of  $V(\tau + 2\tau_1)$  was terminated in fourth order. Any higher-order error terms will presumably contribute to the decay when  $\tau$  becomes several times larger than  $\tau_1$ . However, the data show that  $M_y(t)$  and  $M_x(t)$  are virtually identical.  $\tau_1$  chosen here was apparently short enough to render all error terms ineffective for times of the order of

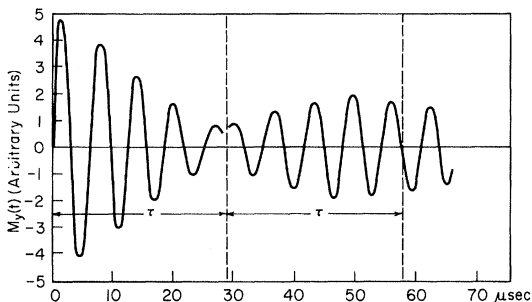


FIG. 5. RSE in Teflon obtained by rf phase reversal at exact resonance [(v) of Sec. III].  $\Delta H_1/H_1 \approx 0.17$ .

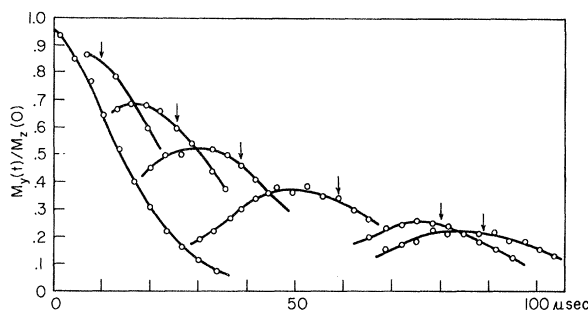


FIG. 6. Group of RSE's at exact resonance [(v) of Sec. III].  $\Delta H_1/H_1 \approx 0.17$ . Circles represent the experimentally observed maxima of  $M_y(t)$  (see Fig. 5), and arrows indicate the expected positions of the echo maxima.

$T_{2p}$  at exact resonance.

(iv) The solid echo generated by the pulse sequence 2(b) has not been fully exploited as yet. Its maximum is given by Eq. (19) which, again, contains an error term damping in fourth order. However, for  $\tau_1 = 0$ , the transverse magnetization in the rotating frame should be completely recovered at time  $\tau/2$  (measured from the end of the second pulse) even for large  $\tau$ 's, as discussed in (i) of Sec. II following Eq. (18). For finite  $\tau_1$  (8  $\mu$ sec), Figs. 4(a) and 4(b) show echoes for  $n = 2$  and 7, respectively, together with the decay curves taken without the refocussing pulse (lower trace). The arrows indicate the theoretically expected positions of the echo maxima. The observed maxima are shifted slightly to the left because of the superimposed near-exponential envelope decay. This is demonstrated in Fig. 4(c) which shows superimposed echoes for values of the integer  $n$  from Eq. (9) varying from 0 to 9. The decay of the echo envelope is thought to be caused mainly by the nonsecular dipolar terms ( $H_1 = 5.7$  G was used) and, to a lesser extent, by rf field inhomogeneities and error-term contributions. For  $n = 9$ , the rf pulse length was about 208  $\mu$ sec so that, under present experimental conditions, an echo at exact resonance could be produced at a time of about  $10T_2$ .

(v) Any magnetic field inhomogeneity at exact resonance can be eliminated by inverting  $H_1$  at the midpoint of the rf pulse, similarly to the technique proposed by Solomon.<sup>11</sup> Two rf pulses separated by about 2  $\mu$ sec and differing in phase by  $180^\circ$  were fed into a single-coil system generating an  $H_1$  field of 39.3 G with an estimated inhomogeneity of about 17% across the sample volume.

Both  $M_y(t)$  and  $M_x(t)$  were recorded as a function of the pulse length. Figure 5 shows the time variation of the transverse magnetization in the rotating frame at exact resonance. The rapid initial decay was obtained by reading the signal amplitude following the first rf pulse. Its time con-

stant is mainly determined by the large rf inhomogeneity. At  $t = \tau$ , the  $180^\circ$ -phase-shifted second pulse was turned on. The first pulse length was kept fixed, and the data were taken by increasing the length of the second pulse. A rotary spin echo (RSE) then appeared. The same process was repeated for different  $\tau$ 's resulting in a group of RSE's shown in Fig. 6. The arrows indicate the theoretically expected positions of the echo maxima at  $t = 2\tau$ . Because of the great amount of rf inhomogeneity introduced, the echoes were well separated. The decay of the RSE envelope is caused predominantly by the secular part of the dipolar Hamiltonian which is, therefore, responsible for the shift of the echo maxima to the left. The data are plotted in Fig. 1 and compared with the results obtained in (i) of Sec. III. The somewhat poor agreement of the various sets of data is believed to be due to the difficulty of normalizing the decays obtained under different experimental conditions as well as to the experimental error in adjusting a phase difference to exactly  $180^\circ$ .

#### IV. SUMMARY

The rotary component of magnetization in the  $x, y$  plane, then, cannot be traced out by recording the height of the FID following the rf pulse because

of the discontinuity of the signal slope at the turning-off point of the pulse. However, this component may be locked by an instantaneous  $90^\circ$  phase shift of the rf field. More importantly, it may be recovered by a  $90^\circ$ -phase-shifted  $90^\circ$  pulse which, ideally, will refocus the entire rotary FID, compressed in time by a factor of 2, provided that (i) the leading rf pulse has length  $\tau = \pi/2 + n\pi$  and (ii) the phase change of the rf field is accomplished instantaneously. This pulse sequence renders the time-development operator equal to unity at time  $\tau + \tau/2$ , so that the echo maxima reproduce the initial magnetization of the isolated spin system independent of  $\tau$ .

These observations clearly contradict the assumption that the spin system has attained a state of internal equilibrium in the presence of a strong rf field. A description of the isolated system in terms of a single-spin temperature would rule out any phase memory and, hence, would not allow a time reversal of supposedly random statistical dipolar couplings. Our experimental results do not quite match the theoretical predictions because we were not able to satisfy condition (ii) above. However, the rotary echo formation is clearly indicated. These ideas are more fully explored in two recent publications<sup>12,13</sup> in which multiple pulse sequences are used rather than continuous rf fields.

\*Work supported by the University of North Carolina Materials Research Center under Contract No. SD-100 from the Advanced Research Projects Agency.

†Present address: Department of Chemistry and Research Laboratory of Electronics, Massachusetts Institute of Technology, Cambridge, Mass. 02139.

<sup>1</sup>W. I. Goldberg and M. Lee, *Phys. Rev. Letters* **11**, 255 (1963).

<sup>2</sup>D. Barnaal and I. J. Lowe, *Phys. Rev. Letters* **11**, 258 (1963).

<sup>3</sup>A. G. Redfield, *Phys. Rev.* **98**, 1787 (1955).

<sup>4</sup>A. Abragam, *The Principles of Nuclear Magnetism* (Oxford U. P., London, 1961).

<sup>5</sup>E. Merzbacher, *Quantum Mechanics* (Wiley, New York, 1962).

<sup>6</sup>J. G. Powles and J. H. Strange, *Proc. Phys. Soc. (London)* **82**, 6 (1963).

<sup>7</sup>P. Mansfield, *Phys. Rev.* **137**, A961 (1965).

<sup>8</sup>S. R. Hartmann and E. L. Hahn, *Phys. Rev.* **128**, 2042 (1962).

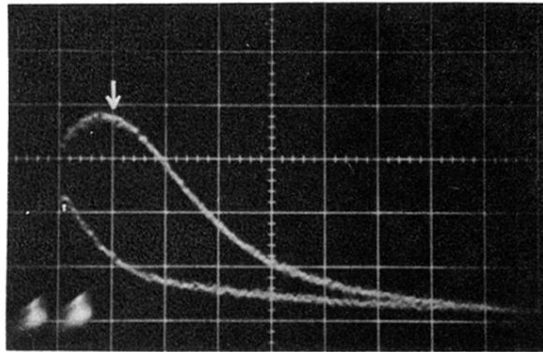
<sup>9</sup>C. P. Slichter and W. C. Holton, *Phys. Rev.* **122**, 1701 (1961).

<sup>10</sup>D. C. Ailion and C. P. Slichter, *Phys. Rev.* **137**, A235 (1965).

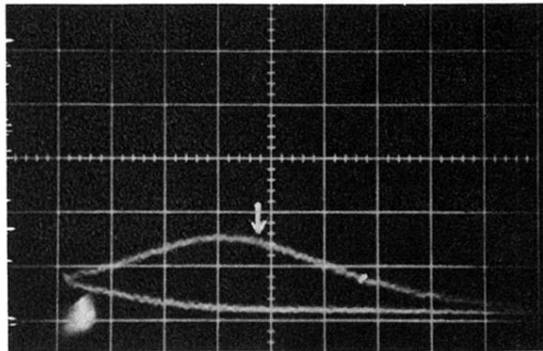
<sup>11</sup>I. Solomon, *Phys. Rev. Letters* **2**, 301 (1959).

<sup>12</sup>W.-K. Rhim, A. Pines, and J. S. Waugh, *Phys. Rev. Letters* **25**, 218 (1970).

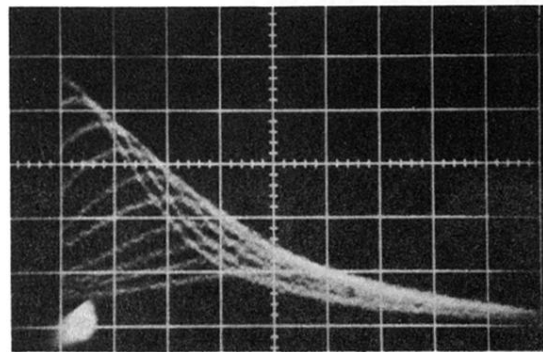
<sup>13</sup>W.-K. Rhim, A. Pines, and J. S. Waugh, *Phys. Rev. B* **3**, 684 (1971).



(a)



(b)



(c)

FIG. 4. Echoes in Teflon at exact resonance generated by pulse sequence of Fig. 2(b) [(iv) of Sec. III]. The oscilloscope sweep rate is  $20 \mu\text{sec/cm}$ . Arrows indicate the theoretically expected positions of the echo maxima. (a) Upper trace: echo for  $n=2$ ; lower trace: signal without refocussing pulse. (b) Upper trace: echo for  $n=7$ ; lower trace: signal without refocussing pulse. (c) Multiple exposure of echoes from  $n=0$  to  $n=9$ .